

Model System of Self-Reproducing Vesicles

Yuka Sakuma and Masayuki Imai*

Department of Physics, Ochanomizu University, Bunkyo, Tokyo 112-8610, Japan

(Received 18 March 2011; published 31 October 2011)

Development of self-reproducing vesicle systems is the first step for autopoietic cycles. We established a model self-reproducing vesicle system without the membrane molecule synthesis route. The model vesicle composed of cylinder- and inverse-cone-shaped lipids formed inclusion vesicles inside the mother vesicle, and the inclusion vesicles were then expelled by a temperature cycling. By changing the vesicle composition, the mother vesicles showed a budding-type self-reproduction pathway. A key concept of this system is the coupling of the main-chain transition and the shape of lipids.

DOI: 10.1103/PhysRevLett.107.198101

PACS numbers: 87.16.D-, 87.14.Cc, 87.17.Ee

Synthesizing simple living cells that contain the minimal elements necessary to perform the basic functions of life will provide insight into the biophysical origins of life [1]. These simple cells are called minimal cells, and the development of a self-reproducing vesicle system is the first step in developing autopoietic cycles [2]. To date, self-reproducing vesicle systems have been realized in membrane synthesis systems by synthetic biologists [3–7]. In a typical self-reproducing vesicle system [7], membrane precursors are converted into membrane molecules with the help of a catalyst, and the membrane molecules assemble to form inclusion vesicles inside the mother vesicle. When the inclusion vesicle grows to a certain size, it is expelled from the mother vesicle in a process called “birthing.” This translocation pathway is frequently observed in self-reproducing vesicle systems and schematically represented in Fig. 1(a). In self-reproducing vesicle systems, another topological transition pathway called the “budding mechanism” has been reported, where the mother vesicle deforms to a pearlike shape and then is divided into two vesicles [Fig. 1(b)] [2].

The self-reproducing vesicle system is caused by a complex interplay between the chemical synthesis and self-assembly systems, and to date we are still far from a simple physical understanding for such mechanisms [2,8,9]. In this Letter, we describe a model system of self-reproducing vesicles without the membrane molecule synthesis route, i.e., no membrane molecule supply route in the system. The model self-reproducing vesicles can reproduce two types of topological transitions: the translocation and the budding mechanisms. Both pathways are controlled by a simple temperature cycling. A key concept of this model self-reproducing vesicle system is the coupling of the main-chain transition and the shape of lipids, which controls the reduced volume of the vesicle, $v = V/[(4\pi/3)(A/4\pi)^{3/2}]$ (V , vesicle volume and A , vesicle area), and the local curvature of the membrane [10–12].

To create the model self-reproducing giant unilamellar vesicle (GUV) system, we used binary vesicles composed

of inverse-cone-shaped lipids [1, 2-dilauroyl-*sn*-glycero-3-phosphoethanolamine (DLPE)] and cylinder-shaped lipids [1, 2-dipalmitoyl-*sn*-glycero-3-phosphocholine (DPPC)]. Lipids with a phosphoethanolamine head group (PE lipids) are frequently observed in topological change of the cellular membrane, i.e., fission and fusion events [13–16], indicating that the PE lipids encourage topological transitions. Phospholipids used in this study were purchased from Avanti Polar Lipid, Inc. (Alabaster, AL) and used without further purification. The main-chain transition of the lipids was examined by using a differential scanning calorimetry apparatus (Seiko DSC6100). The main-chain transition temperatures of DPPC and DLPE were $T_m^{\text{DPPC}} = 41^\circ\text{C}$ and $T_m^{\text{DLPE}} = 29^\circ\text{C}$, respectively. It should be noted that the main-chain transition temperature of DPPC and DLPE mixed membrane changed as follows: 39°C (DPPC/DLPE = 8/2, molar ratio), 35.5°C (7/3), 33.5°C (5/5), and 32°C (3/7). Texas red-1, 2-dihexadecanoyl-*sn*-glycero-3-phosphoethanolamine was obtained from Molecular Probes (Eugene, OR) and used as a dye for membranes. Binary GUVs were prepared by using a gentle hydration method [17,18]. The GUV deformation caused by cycling the temperature between 35 and 42°C

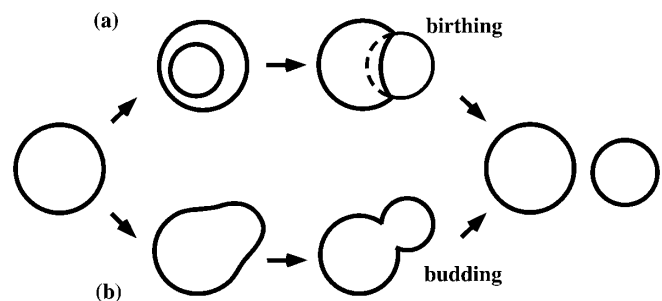


FIG. 1. A schematic representation of self-reproducing vesicle pathways. (a) Translocation: An inclusion vesicle is formed inside the mother vesicle and then expelled from the mother vesicle in a process called birthing. (b) Budding: The mother vesicle deforms to a pearlike shape and then is divided into two vesicles.

was followed by using a fluorescence microscope (Carl Zeiss, Axioskop 40) with a CCD camera (Carl Zeiss, Axio Cam MRc 5). We also examined the similar self-reproducing pathway of binary GUVs containing other types of PE lipids: 1, 2-dimyristoyl-*sn*-glycero-3-phosphoethanolamine and 1, 2-dipalmitoyl-*sn*-glycero-3-phosphoethanolamine.

The observed translocation pathway in binary GUVs with a composition of DLPE/DPPC = 3/7 is shown in Fig. 2 [19]. We prepared binary GUVs at 60 °C, above T_m^{DPPC} , and then decreased the temperature (T) to 35 °C, where the GUV had a spherical shape (step 1, Fig. 2A). By increasing the temperature to 42 °C, chain melting took place, which produced the excess area [12]. By using the excess area, the spherical GUV deformed to a stomatocyte shape (step 2, Fig. 2B–C). With the elapse of time, the stomatocyte vesicle formed an inclusion vesicle inside the mother vesicle spontaneously by pinching off the invagination neck (step 3, Fig. 2D–F). When the temperature was decreased from 42 to 35 °C, the surface area of the mother vesicle decreased due to the chain ordering. This resulted in an increase in the inner pressure of the mother vesicle. In order to release the inner pressure, the mother vesicle formed a single pore and the inclusion vesicle was discharged through the pore with the interior solution [12], i.e., birthing of the daughter vesicle (step 4, Fig. 2G–I) [3,4]. After the birthing, the pore was immediately resealed due to the line tension, and the mother GUV recovered the spherical shape (Fig. 2J) although the resulting GUV had a smaller size than the original GUV; i.e., the averaged mother to daughter vesicle size ratio at this vesicle

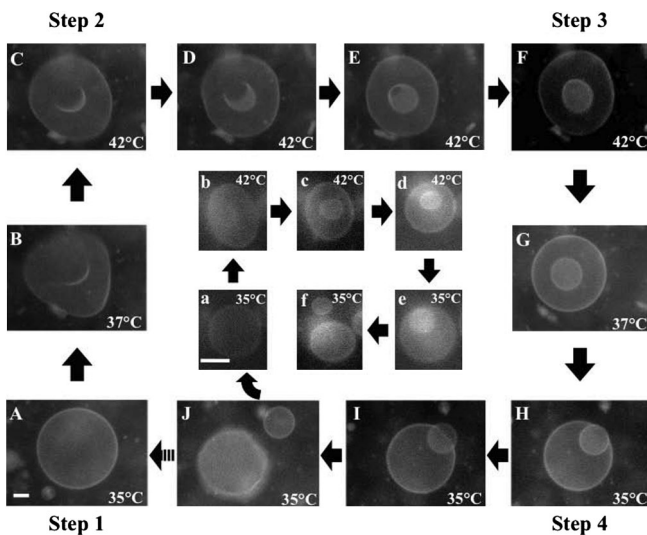


FIG. 2. A series of snapshots in the translocation process is shown in A–J. The translocation cycle consists of four steps: (i) sphere to stomatocyte deformation (A–C), (ii) formation of the inclusion vesicle (D–F), (iii) birthing of the daughter vesicle through a pore (G–I), and (iv) recovery of the spherical vesicle by closing the pore (J). a–f show the translocation cycle of the daughter vesicle. The scale bar indicates 5 μm .

composition was ca. 0.4. We examined ca. 50 binary GUVs subjected to the temperature cycle, and ca. 90% of GUVs having the diameter of 20–100 μm showed the translocation pathway.

Interestingly, when the temperature was again increased to 42 °C, the recovered spherical mother GUVs formed inclusion vesicles, and then the second daughter vesicles were born by decreasing the temperature to 35 °C. Thus the binary GUV composed of DLPE and DPPC repeated the translocation pathway when the temperature was cycled. In addition, the daughter vesicle followed the same translocation pathway and often produced granddaughter vesicles (Fig. 2a–f). This indicates that the birthing ability is maintained beyond a single generation (sometimes we obtained fourth- or fifth-generation vesicles). These unique self-similar birthing dynamics, which were realized by using a simple heat cycle without the synthesis routine, makes the physical aspects of the self-reproducing vesicle system clear. Pure DPPC GUVs without DLPE showed the deformation to the stomatocyte vesicle but no transformation to the inclusion vesicle by pinching off the neck. This strongly suggests that the DLPE brings the topological transition.

In order to reveal a role of DLPE in the topological transition, we investigated the shape deformation pathways of the binary GUV as a function of the molar fraction of DLPE, $\phi = n_{\text{DLPE}}/n$ (n and n_{DLPE} are the number of total lipids and DLPE lipids in a vesicle, respectively). Figure 3 shows the observed shape deformation pathways (steps 1–4) in a temperature cycle between low annealing temperature $T_L = 35$ °C and high annealing temperature $T_H = 42$ °C. For GUVs with $\phi = 10\%$, the initial spherical GUVs (step 1) deformed to the stomatocyte shape (step 2) and formed a nested vesicle connected to the mother vesicle through a small neck (step 3). When we decreased the temperature to 35 °C, the vesicle returned to the initial spherical shape through the stomatocyte shape (step 4). By temperature cycling the GUVs with $\phi = 10\%$ repeated, this sphere-nested vesicle deformations.

For $15 \leq \phi < 30\%$, the GUVs showed the budding pathways depicted in Fig. 1(b). By increasing the temperature from $T_L = 35$ °C to $T_H = 42$ °C, the spherical GUVs showed outer budding deformations (step 2), and then the buds were completely pinched off; i.e., daughter vesicles were produced by the budding pathway (step 3) [4]. By decreasing the temperature, the mother and the daughter vesicles recovered a spherical shape (step 4). When we performed the second temperature cycling, the mother GUVs repeated the budding pathway and produced the second daughter vesicles, and the first daughter vesicles produced the granddaughter vesicles by the budding pathway. The budding ability was also maintained beyond a single generation and not mixed with the translocation pathway by multitemperature cyclings.

For $30 \leq \phi \leq 45\%$, the GUVs showed the translocation pathway. At $\phi = 30\%$ and 35%, most of the mother

vesicles produced one or two daughter vesicles, whereas at $\phi = 40\%$, the mother vesicles formed many inner buds, identical to forming many inclusion vesicles. By decreasing the temperature, several inclusion vesicles were expelled from the mother vesicle, and the remaining vesicles stayed inside the mother vesicle. When we increased the DLPE molar fraction more than 50%, the binary GUVs showed no production of daughter vesicles.

The dynamical morphology transition behaviors of binary GUVs composed of DLPE and DPPC (Fig. 3) strongly suggest that the two types of self-reproducing pathways, translocation and budding, can be controlled by the content of DLPE. In other words, DLPE plays an important role in the topological transition of vesicle division, which is consistent with the observations in cell divisions [13–16]. Actually, the translocation and the budding vesicle pathways were observed in binary GUVs containing other types of PE lipids. These binary systems included 1, 2-dimyristoyl-*sn*-glycero-3-phosphoethanolamine/DPPC and 1, 2-dipalmitoyl-*sn*-glycero-3-phosphoethanolamine/DPPC. These self-reproducing vesicle phenomena were not observed in the binary GUVs composed of cylinder and cylinder-shaped lipids [11] and cone- and cylinder-shaped lipids [12].

Key points of the model self-reproducing vesicles composed of cylinder-shaped and PE lipids are (i) fission of the vesicle, (ii) continuous formation of new-generation vesicles by temperature cycling, and (iii) control of the

budding and the translocation pathways. Here we propose the following interpretations for the observed features.

(i) *Fission of vesicles.*—It is well known that the neck connecting mother and daughter vesicles is astonishingly stable and the phase separation on the vesicle drives the fission of vesicles by using the line tension [20–23]. In order to eliminate the contribution of the phase separation to the observed fission, we increased T_H to 50 °C, which is sufficiently high compared to the chain melting temperature of DPPC, $T_m^{\text{DPPC}} = 41$ °C. In this temperature cycling, the mother vesicle formed an inclusion vesicle and expelled it through the pore, indicating that the fission took place at 50 °C. Actually, in the fluorescence images (Figs. 2 and 3) we observed no domain formation during the temperature cycles. Thus, the fission takes place in the one-phase region.

A plausible explanation for the observed fission is the local phase separation of PE lipids at the neck, which destabilize the neck due to the spontaneous curvature of the lipids [21]. From a theoretical point of view, Chen, Higgs, and MacKintosh showed that the coupling between Gaussian curvature and local lipid composition for two component vesicles can destabilize the narrow neck in the fluid phase [22]. In the fission process, the size of the neck reaches a few tens of nanometers. The large membrane curvature couples with the spontaneous curvature of PE lipids, which modifies the local lipid composition at the neck, so-called lipid sorting [24,25]. The lipid sorting has been reported for the lipid bilayers with the curvature of $\sim 1/20$ nm⁻¹ [25,26]. Unfortunately, it was very hard to detect the local phase separation at the neck experimentally; however, local segregation might occur at the narrow neck with the scale of a few tens of nanometers.

(ii) *Continuous formation of vesicles.*—The continuous formation of new-generation vesicles by temperature cycling indicates that the new-generation vesicles have the same composition as the mother vesicles. We examined the composition change of vesicles during the vesicle division based on the fact that the main-chain transition temperature of the DLPE or DPPC binary vesicle depends on the composition. The differential scanning calorimetry profiles showed that during the multitemperature cycles the peak profiles kept a constant shape and no main-chain transition temperature change was detected for the budding and the translocation pathways. Thus the mother and the daughter vesicles have the same composition. It should be noted that the effect of the local segregation at the neck on the bulk composition might be negligible.

(iii) *Budding and translocation pathways.*—The binary GUVs showed outward budding for $15 \leq \phi < 30\%$ and inward budding for $30 \leq \phi \leq 45\%$. Here we discuss the observed shape deformations based on the area difference elasticity model [27,28]. The area difference elasticity model shows that the morphology of the vesicle is determined by the reduced volume v and the intrinsic area

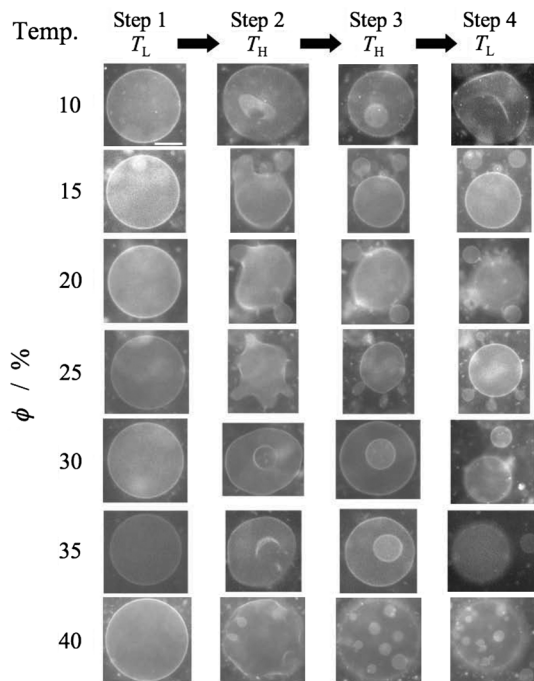


FIG. 3. Dynamical morphology diagram in a temperature cycling (steps 1–4) is summarized as a function of the DLPE molar fraction. The scale bar is 10 μm .

difference $\Delta A_0 = (n^{\text{out}} - n^{\text{in}})a_0$, where a_0 is the cross-section area of a lipid and n^{out} and n^{in} are the number of lipids in outer and inner leaflets, respectively. The area difference elasticity model shows that the pear-shaped vesicle (outward budding) is stable in the region of $0.7 < \nu < 0.9$ and $1.5 < \Delta A_0/(8\pi dR_{\text{in}}) < 1.7$, whereas the stomatocyte-shaped vesicle (inward budding) is stable in the region of $0.7 < \nu < 0.9$ and $0.4 < \Delta A_0/(8\pi dR_{\text{in}}) < 0.8$. We calculate the change of the reduced volume and the intrinsic area difference of the spherical vesicle (inner radius of R_{in} and bilayer thickness of $2d$) induced by the chain melting.

At the initial stage ($T = T_L$), the binary vesicle has a spherical shape. Using cross-section areas of a DLPE lipid, a_{DLPE} , and a DPPC lipid in the ordered state, a_{DPPC} , we can express the surface area of inner and outer leaflets by $A^{\text{in}} = [a_{\text{DLPE}}\phi^{\text{in}} + a_{\text{DPPC}}(1 - \phi^{\text{in}})]n^{\text{in}} = 4\pi R_{\text{in}}^2$ and $A^{\text{out}} = [a_{\text{DLPE}}\phi^{\text{out}} + a_{\text{DPPC}}(1 - \phi^{\text{out}})]n^{\text{out}} = 4\pi(R_{\text{in}} + d)^2$, respectively, where the molar fraction of DLPE in the inner and the outer leaflets is expressed by $\phi^{\text{in}} = n_{\text{DLPE}}^{\text{in}}/n^{\text{in}}$ and $\phi^{\text{out}} = n_{\text{DLPE}}^{\text{out}}/n^{\text{out}}$, respectively (n_{DLPE}^i , the number of DLPE lipids in the i leaflet, $i = \text{in or out}$). For simplicity, we assume $a_{\text{DLPE}} = a_{\text{DPPC}} = a$. Then the reduced volume and the intrinsic area difference of the spherical vesicle are expressed by $\nu = 1$ and $\Delta A_0 \cong 8\pi R_{\text{in}}d$, respectively.

When we increase the temperature to T_H , the chain melting of DPPC takes place, which increases a cross-section area of a DPPC lipid about 40%, i.e., $a \rightarrow 1.4a$ [12,29]. Then the surface area of the GUV increases with keeping the vesicle volume constant. Using the excess area, the GUV deforms to the pear shape or the stomatocyte shape depending on the DLPE fraction. A simple geometrical calculation shows that, by chain melting, the reduced volume decreases to $\nu = (1.4 - 0.4\phi^{\text{in}})^{-3/2}$ and the intrinsic area difference changes to $\Delta A_0/(8\pi dR_{\text{in}}) = 1.4 - 0.4\phi + (R_{\text{in}}/d)(\phi^{\text{in}} - \phi)$. The decrease of the reduced volume ($\nu = 0.6-0.7$ for $\phi^{\text{in}} = 0.2-0.5$) is consistent with the observed vesicle deformations. On the other hand, the change of the intrinsic area difference strongly depends on the asymmetric transversal distribution of DLPE in the bilayer, $\phi^{\text{in}} - \phi$, since the GUV has a very large value of $R_{\text{in}}/d \sim 5000$. Thus a very little asymmetric transversal distribution of lipids in the bilayer governs the deformation pathway. We consider that the distribution depends on the composition of the binary GUV.

In conclusion, by coupling the PE lipids and the main-chain transition of DPPC, we demonstrated a model self-reproducing vesicle system, where the vesicles continuously formed new-generation vesicles with identical composition by temperature cycling. The new-generation vesicles were produced by the budding and the translocation (birthing) pathways depending on the molar fraction of PE lipids. The local phase separation at the neck caused by the coupling between the membrane curvature and the lipid geometry might be responsible for the observed shape

deformations. This model system without the synthesis routine sheds light on the physical aspects of the self-reproducing vesicle systems, although we still have a long distance to the autopoietic cycles.

The authors are grateful to T. Sugawara (The University of Tokyo), T. Taniguchi (Kyoto University), and P. Zihler (Jozef Stefan Institute) for valuable discussion of the experimental results. This work was supported by KAKENHI (Grant-in-Aid for Scientific Research) on Priority Area ‘‘Soft Matter Physics’’ from the Ministry of Education, Culture, Sports, Science and Technology of Japan and Grant-in-Aid for Scientific Research (A) No. 22244053 from the Japan Society for the Promotion of Science. Y. S. thanks Japan Society for the Promotion of Science, Grant-in-Aid for JSPS Fellows (No. 20-2802) for support.

*To whom all correspondence should be addressed.

- [1] J. W. Szostak, D. P. Bartel, and P. L. Luisi, *Nature (London)* **409**, 387 (2001).
- [2] P. Stano and P. L. Luisi, *Chem. Commun. (Cambridge)* **46** (2010) 3639.
- [3] F. M. Menger and K. J. Gabrielson, *J. Am. Chem. Soc.* **116**, 1567 (1994).
- [4] R. Wick, P. Walde, and P. L. Luisi, *J. Am. Chem. Soc.* **117**, 1435 (1995).
- [5] M. M. Hanczyz, S. M. Fujikawa, and J. W. Szostak, *Science* **302**, 618 (2003).
- [6] K. Takakura, T. Toyota, and T. Sugawara, *J. Am. Chem. Soc.* **125**, 8134 (2003).
- [7] K. Takakura and T. Sugawara, *Langmuir* **20**, 3832 (2004).
- [8] F. M. Menger and M. I. Angelova, *Acc. Chem. Res.* **31**, 789 (1998).
- [9] B. Bozic and S. Svetina, *Eur. Biophys. J.* **33**, 565 (2004).
- [10] Y. Sakuma, M. Imai, M. Yanagisawa, and S. Komura, *Eur. Phys. J. E* **25**, 403 (2008).
- [11] M. Yanagisawa, M. Imai, and T. Taniguchi, *Phys. Rev. Lett.* **100**, 148102 (2008).
- [12] Y. Sakuma, T. Taniguchi, and M. Imai, *Biophys. J.* **99**, 472 (2010).
- [13] K. Emoto, T. Kobayashi, A. Yamaji, H. Aizawa, I. Tahara, K. Inoue, and M. Umeda, *Proc. Natl. Acad. Sci. U.S.A.* **93**, 12 867 (1996).
- [14] D. P. Siegel and M. M. Kozlov, *Biophys. J.* **87**, 366 (2004).
- [15] T. Kaasgaard and C. J. Drummond, *Phys. Chem. Chem. Phys.* **8**, 4957 (2006).
- [16] I. M. Hafez and P. R. Cullis, *Adv. Drug Delivery Rev.* **47**, 139 (2001).
- [17] J. P. Reeves and R. M. Dowben, *J. Cell. Physiol.* **73**, 49 (1969).
- [18] D. Needham and E. Evans, *Biochemistry* **27**, 8261 (1988).
- [19] See Supplemental Material at <http://link.aps.org/supplemental/10.1103/PhysRevLett.107.198101> for self-birthing vesicle.
- [20] R. Lipowsky, *J. Phys. II (France)* **2**, 1825 (1992).
- [21] H.-G. Döbereiner, J. Käs, D. Noppi, I. Sprenger, and E. Sackmann, *Biophys. J.* **65**, 1396 (1993).

- [22] C.-M. Chen, P. G. Higgs, and F. C. MacKintosh, *Phys. Rev. Lett.* **79**, 1579 (1997).
- [23] M. Andes-Koback and C. D. Keating, *J. Am. Chem. Soc.* **133**, 9545 (2011).
- [24] A. Tian and T. Baumgart, *Biophys. J.* **96**, 2676 (2009).
- [25] M. M. Kamal, D. Mills, M. Grzybek, and J. Howard, *Proc. Natl. Acad. Sci. U.S.A.* **106**, 22 245 (2009).
- [26] Y. Sakuma, N. Urakami, T. Taniguchi, and M. Imai, *J. Phys. Condens. Matter* **23**, 284104 (2011).
- [27] U. Seifert, K. Berndl, and R. Lipowsky, *Phys. Rev. A* **44**, 1182 (1991).
- [28] B. Bozic, S. Sventina, B. Zeks, and R. E. Waugh, *Biophys. J.* **61**, 963 (1992).
- [29] J. F. Nagle and S. Tristram-Nagle, *Biochim. Biophys. Acta* **1469**, 159 (2000).